Computational Structural Engineering
An International Journal
Vol. 3, No. 1, pp. 61~68 (2003)

Computational Structural Engineering Institute

Wind-Induced Vibration Control of a Tall Building Using Magneto-Rheological Dampers: A Feasibility Study

Ja-In Gu[1], Saang Bum Kim[†], Chung-Bang Yun[2] and Yun-Seok Kim[3]

[1]*Researcher, Samsung Data System*
[†]*Visiting Scholar, University of Illinois at Urbana and Champaign,*
[2]*Member, Professor, Korea Advanced Institute of Science and Technology,*
[3]*Member, Researcher, Hyundai Institute of Construction Technology*

Received November 2002; Accepted November 2003

ABSTRACT

A recently developed semi-active control system employing magneto-rheological (MR) fluid dampers is applied to vibration control of a wind excited tall building. The semi-active control system with MR fluid dampers appears to have the reliability of passive control devices and the adaptability of fully active control systems. The system requires only small power source, which is critical during severe events, when the main power source may fail. Numerical simulation studies are performed to demonstrate the efficiency of the MR dampers on the third ASCE benchmark problem. Multiple MR dampers are assumed to be installed in the 76-story building. Genetic algorithm is applied to determine the optimal locations and capacities of the MR dampers. Clipped optimal controller is designed to control the MR dampers based on the acceleration feedback. To verify the robustness with respect to the variation of the external wind force, several cases with different wind forces are considered in the numerical simulation. Simulation results show that the semi-actively controlled MR dampers can effectively reduce both the peak and RMS responses the tall building under various wind force conditions. The control performance of the MR dampers for wind is found to be fairly similar to the performance of an active tuned mass damper.

Keywords: semi-active control, magneto-rheological dampers, wind vibration, tall building

1. Introduction

Slender and tall buildings are very sensitive to wind loads. To enhance the human comfort under wind loads, tuned mass dampers and active tuned mass dampers have been widely used for response control of wind excited tall buildings (Yang and Samali, 1983; Koh *et al.*, 1998; Kim and Yun, 2000). Generally, active control devices require large control forces and a high power supply system to reduce the vibration effectively. However, the active system may not be reliable due to the potential power failure particularly during severe events. Recently, to overcome the weakness of the active control, semi-active control devices were suggested by many researchers (Yang *et al.*, 1983; Fujino *et al.*, 1996; Spencer *et al.*, 1997). Semi-active control uses the passive control device of which the characteristics can be modified adaptively. Control force of the semi-active device is not generated from the actuator with power supply. It is generated as a dynamic reaction force of the device as in the passive control case, so the control system is inherently stable and robust. However, unlike the case of passive control, the control force can be adjusted by tuning the characteristics of the device based on the measured response of the structure, so the vibration can be reduced more effectively under wide range of the external loads.

In this study, a recently developed semi-active control system using MR dampers is applied to control the wind-induced vibration of tall buildings. A numerical simulation study is carried out on a 76-story building, which was proposed for benchmark studies on control of wind-induced vibration by ASCE. Genetic algorithm is used to determine the optimal locations and capacities of the MR dampers. The performance of the semi-actively controlled

[†] Corresponding author
Tel: +1-217-244-9327, Fax: +1-425-871-2170
E-mail address: saangkim@uiuc.edu

case is compared with those of the passively and actively controlled cases, and the effectiveness of the semi-actively controlled MR dampers is discussed.

2. Model of Control System

2.1. Modeling of Structure

Referring to the 76-story building structure for the ASCE benchmark problem of wind vibration control as in Figure 1, the dynamic behavior of the structure with a set of MR dampers can be modeled as:

$$\boldsymbol{M}_s\ddot{\boldsymbol{y}}_s(t)+\boldsymbol{C}_s\dot{\boldsymbol{y}}_s(t)+\boldsymbol{K}_s\boldsymbol{y}_s(t)=\boldsymbol{f}_{sw}(t)+\boldsymbol{B}_{sd}\boldsymbol{f}_{MR}(t,\boldsymbol{v}_c(t)) \quad (1)$$

where $\boldsymbol{y}_s(t),\boldsymbol{f}_{sw}(t),\boldsymbol{f}_{MR}(t,\boldsymbol{v}_c(t))$, and $\boldsymbol{v}_c(t)$ are the vector for the displacement of the structure, the external environmental force by wind, the force from the MR dampers, and the control input voltage applied to the MR dampers; $\boldsymbol{M}_s$, $\boldsymbol{C}_s$, and $\boldsymbol{K}_s$ are the mass, damping, and stiffness matrices of the structure; and $\boldsymbol{B}_{sd}$ is a Boolean matrix representing the effects on the structural responses due to the MR dampers.

The problem organizer constructed a reduced system with 23 DOF's using the state order reduction method for computational efficiency. The selected DOFs are the horizontal displacements of 23 floors: i.e. 3, 6, 10, 13, 16, 20, 23, 26, 30, 33, 36, 40, 43, 46, 50, 53, 56, 60, 63, 66, 70, 73 and 76th floors. The corresponding state and measurement equations are

$$\begin{aligned}\dot{\boldsymbol{x}}(t) &= \boldsymbol{A}\boldsymbol{x}(t)+\boldsymbol{B}_d\boldsymbol{f}_{MR}(t,\boldsymbol{v}_c(t))+\boldsymbol{B}_d\boldsymbol{f}_{ew}(t)\\ \boldsymbol{y}_c(t) &= \boldsymbol{C}_c\boldsymbol{x}(t)+\boldsymbol{D}_{cd}\boldsymbol{f}_{MR}(t,\boldsymbol{v}_c(t))+\boldsymbol{D}_{ce}\boldsymbol{f}_{ew}(t)\\ \boldsymbol{y}_m(t) &= \boldsymbol{C}_m\boldsymbol{x}(t)+\boldsymbol{D}_{md}\boldsymbol{f}_{MR}(t,\boldsymbol{v}_c(t))+\boldsymbol{D}_{me}\boldsymbol{f}_{ew}(t)+\boldsymbol{v}_m(t)\end{aligned} \quad (2)$$

where $\boldsymbol{x}(t),\boldsymbol{f}_{ew}(t),\boldsymbol{y}_c(t),\boldsymbol{y}_m(t)$ and $\boldsymbol{v}_m(t)$ are the state vector, the disturbance vector including effects of wind force, an output vector for control objective, another output vector for measurement, and the measurement noise vector; and $\boldsymbol{A},\boldsymbol{B}_d,\boldsymbol{B}_e,\boldsymbol{C}_c,\boldsymbol{D}_{cd},\boldsymbol{D}_{ce},\boldsymbol{C}_m,\boldsymbol{D}_{md}$ and $\boldsymbol{D}_{me}$ are system matrices.

2.2. Model of MR Fluid Damper

The MR fluid damper has several unique characteristics, such as high dynamic yield strength, wide operating temperature range, requirement of small voltage to control the damper force, and short response time (Carlson *et al.*, 1994). Many researchers studied on modeling of the MR fluid damper. In this paper, the bi-viscous model shown in Figure 2 (Stanway *et al.* 1996) is used to predict the behavior of the MR damper. Then the damper force can be modeled as:

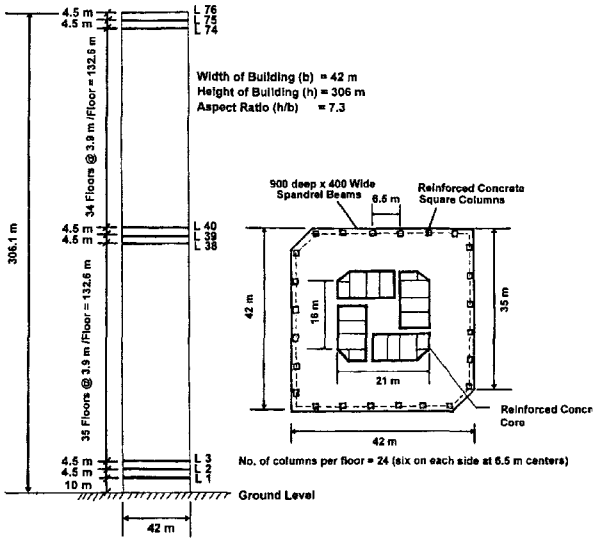

Fig. 1. Benchmark Structure for Wind Vibration Control

$$f_{MR,i}(t)=\begin{cases} c_{0,i}\dot{y}_{MR,i}(t), & \text{if } |\dot{y}_{MR,i}(t)|<\dot{y}_{MRy} \\ c_1(\dot{y}_{MR,i}(t)-\dot{y}_{MRy})+f_{MRy,i}sgn(\dot{y}_{MR,i}(t)), & \text{if } |\dot{y}_{MR,i}(t)|\geq\dot{y}_{MRy}\end{cases} \quad (3)$$

where $f_{MR,i}(t)$ is the force of the i-th MR damper, $\dot{y}_{MR,j}(t)$ is the velocity of the i-th MR damper, is the yield velocity of the MR damper, $f_{MRy,i}$ is the yield force of the i-th MR damper; $c_{0,i}$ and c_1 are the damping coefficients of the i-th MR damper for pre- and post-yield conditions.

Damping characteristics of the MR damper can be controlled by the applied current $u_{MR,i}(t)$ into the i-th MR dampers, which can change the intensity of the magnetic field on the MR fluids. The functional dependence of the bi-viscous parameters of the MR dampers on the applied

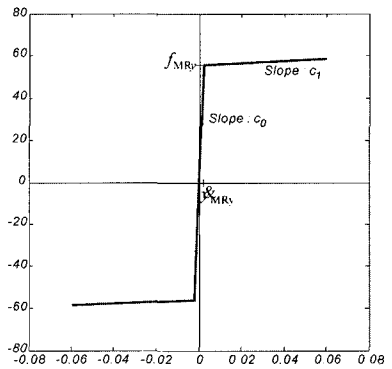

Fig. 2. Bi-Viscous Model for the MR Damper

:urrent $u_{MR,i}(t)$ is considered as follows (Dyke *et al.*, 1998):

$$f_{MRy,i}(t,u_{MR,i}(t)) = f_{MRyb} + f_{MRya}u_{MR,i}(t)$$
$$c_{0,i}(t,u_{MR,i}(t)) = c_{ob} + c_{oa}u_{MR,i}(t) \quad (4)$$

The applied current $u_{MR,i}(t)$ into the i-th MR dampers is :ontrolled by the i-th control input voltage $v_{c,i}(t)$ through he current driver, which is modeled as a first order filter Spencer *et al.*, 1997)

$$\dot{u}_{MR,i}(t) = -\frac{1}{\eta}u_{MR,i}(t) + k_{av}\upsilon_{c,i}(t) \quad (5)$$

where is η the time constant of the filter, k_{av} is the filter gain of the current driver.

The MR dampers with a capacity of 200 kN and a lynamic ratio of 10 for each unit, which were designed by Lord Corporation and tested at University of Notre Dame Spencer *et al.*, 1997), are selected for this study. Damper parameters are shown in Table 1.

2.3. Model Reduction and State Observer

Before designing the controller, two stages of predesign were carried out. The first stage is for another model reduction from 23 DOFs to 5 DOFs for the computational efficiency in the control process. The DOFs of the reduced system are the horizontal displacements of 16, 30, 40, 60 and 76th floors. The second is for design of observer. The Kalman-Bucy filter is used to estimate the state from the measured signal as (Goodwin and Sin 1984):

$$\dot{\hat{x}}_r(t) = \boldsymbol{A}_r\hat{\boldsymbol{x}}_r(t) + \boldsymbol{B}_{rd}\boldsymbol{f}_{MR}(t) + \boldsymbol{L}_{obs}(\boldsymbol{y}_m(t) - \boldsymbol{C}_{mr}\hat{\boldsymbol{x}}_r(t) - \boldsymbol{D}_{mrd}\boldsymbol{f}_{MR}(t)) \quad (6)$$

where $\hat{\boldsymbol{x}}_r(t)$ is the estimated state vector; $\boldsymbol{y}_m(t)$is the measured output vector, $[\boldsymbol{y}_{s50}, \boldsymbol{y}_{s70}, \boldsymbol{y}_{s76}]^T$; $\boldsymbol{A}_r$, $\boldsymbol{B}_{rd}$, $\boldsymbol{B}_{re}$, $\boldsymbol{C}_{mr}$, $\boldsymbol{D}_{mrd}$, and $\boldsymbol{D}_{mre}$ are the reduced system matrices; $\boldsymbol{L}_{obs} = (\boldsymbol{P}_{obs}\boldsymbol{C}_{mr}^T + \boldsymbol{S}_{obs})\boldsymbol{R}_{obs}^{-1}$ is the observer gain matrix, which can be obtained by solving the following algebraic Riccati equatioin for $\boldsymbol{P}_{obs}$:

Table 1. Parameters of the Bi-Viscous Model

Parameter	Value	Parameter	Value
f_{MRya}	90 kN/A	f_{MRyb}	20 kN
c_{oa}	45000 kNs/m/A	c_{ob}	10000 kNs/m
c_1	50 kNs/m	y_{MRy}	0.002 m/s
η	0.002 sec	k_{av}	0.4 A/V

$$\bar{\boldsymbol{A}}_r\boldsymbol{P}_{obs} + \boldsymbol{P}_{obs}\bar{\boldsymbol{A}}_r^T - \boldsymbol{P}_{obs}\boldsymbol{C}_{mr}^T\boldsymbol{R}_{obs}^{-1}\boldsymbol{C}_{mr}\boldsymbol{P}_{obs} + \boldsymbol{Q}_{obs} - \boldsymbol{S}_{obs}\boldsymbol{R}_{obs}^{-1}\boldsymbol{S}_{obs}^T = 0 \quad (7)$$

where $\bar{\boldsymbol{A}}_r = \boldsymbol{A}_r - \boldsymbol{C}_{obs}^T\boldsymbol{R}_{obs}^{-1}\boldsymbol{S}_{obs}^T$;

$$\begin{bmatrix}\boldsymbol{Q}_{obs} & \boldsymbol{R}_{obs}\\ \boldsymbol{R}_{obs} & \boldsymbol{S}_{obs}\end{bmatrix}\delta(t) = E\left\{\begin{bmatrix}\boldsymbol{B}_{rd}\boldsymbol{f}_{ewr}(t)\\ \boldsymbol{D}_{mrd}\boldsymbol{f}_{ewr}(t) + \boldsymbol{v}_m(t)\end{bmatrix}\begin{bmatrix}\boldsymbol{B}_{rd}\boldsymbol{f}_{ewr}(t)\\ \boldsymbol{D}_{mrd}\boldsymbol{f}_{ewr}(t) + \boldsymbol{v}_m(t)\end{bmatrix}^T\right\}$$

; $E\{\}$is the expectation operator; $\boldsymbol{f}_{ews}(t)$ is the disturbance vector for the reduced system including the effects of wind force.

3. Design of Controller

3.1. Clipped Optimal Control for MR Dampers

Conventional control algorithms based on the ordinary linear optimal control have inherent limitations for applying to the semi-active control. Hence, the clipped optimal control proposed for semi-active control system by Sack & Patten (1994) and Dyke *et al.* (1998) is employed in this study. To calculate the desired optimal control force $\boldsymbol{f}_{LQG}(t)$, a linear optimal controller is designed using the linear quadratic Gaussian control theory based on the measured structural acceleration $\boldsymbol{y}_m(t)$ and the measured damper force $\boldsymbol{f}_{MR}$(t) as:

$$\boldsymbol{f}_{LQG}(t) = L^{-1}\left\{\boldsymbol{K}_{LQG}(s)L\left\{\begin{bmatrix}\boldsymbol{y}_m(t)\\ \boldsymbol{f}_{mr}(t)\end{bmatrix}\right\}\right\} \quad (8)$$

where $L\{\}$ is the Laplace transform operator; $\boldsymbol{K}_{LQG}(s)$ is the transfer function of the ordinary LQG controller. The state feedback LQG controller is obtained by minimizing the equation objective function.

$$J = \lim_{t\to\infty}\frac{1}{t}E[\boldsymbol{y}_c^T(t)\boldsymbol{Q}_{LQG}\boldsymbol{y}_c(t) + \boldsymbol{f}_{MR}^T(t)\boldsymbol{R}_{LQG}\boldsymbol{f}_{MR}(t)]dt \quad (9)$$

in which the control variables are taken as $\boldsymbol{y}_c$(t) = [y_{s3}, y_{s30}, y_{s50}, y_{s56}, y_{s60}, y_{s66}, y_{s70}, y_{s73}, y_{s76}]^T; $\boldsymbol{Q}_{LQG}$ is taken as a (9 × 9) diagonal matrix with $\boldsymbol{Q}_{LQG}(i,i)$ = 10 for i = 1, ... 5, and $\boldsymbol{Q}_{LQG}(i,i)$ = 50 for i = 6, ... 9; and $\boldsymbol{R}_{LQG}$ is taken as a (5 × 5) diagonal matrix with $\boldsymbol{R}_{LQG}(i,i) = 1 \times 10^{-7}$ for i = 1, ... 5.

The force generated by the MR damper cannot be directly controlled to get the desired optimal control force $\boldsymbol{f}_{LQG}$, only the command voltage to the MR damper $\boldsymbol{v}_c(t)$ can be directly controlled to increase or decrease the force produced by the device. Hence, to induce the MR damper

to generate approximately the desired optimal control force, the voltage is selected as follows: If the device generates the desired optimal control force (i.e. $f_{MR}(t) = f_{LQG}(t)$), the command voltage remains at the present level. However, if $f_{MR}(t)$ is smaller than $f_{LQG}(t)$ and their signs are same, $v_c(t)$ increases to the maximum level to make $f_{MR}(t)$ increase. Otherwise, the command voltage is set to zero. This algorithm can be expressed using Heaviside step function as (Dyke *et al.*, 1998).

$$v_c(t) = \upsilon_{max} H\{(f_{LQG}(t) - f_{MR}(t)) f_{MR}(t)\} \tag{10}$$

where $H\{\}$ is the Heaviside step function, υ_{max} is the maximum voltage into the current driver for the control of MR damper.

A schematic diagram of the present clipped optimal controller is shown in Figure 3.

3.2. Design of Locations and Capacities of MR Dampers by Genetic Algorithm

The performance of the MR dampers depends strongly on their locations in the structure. The determination of the locations and capacities (numbers of units) of the MR dampers is an integer programming, which requires extensive search and heavy computational efforts. Moreover, the total number of the possible locations is so great for the 76-story building and the cost surfaces may be extremely complex. The genetic algorithm has some advantages that match well with the present problem such as, (1) it optimizes with continuous or discrete parameters; (2) it does not require derivative information; (3) it deals with a large number of parameters; (4) it optimizes parameters with extremely complex cost surfaces; and (5) it can jump out of a local optimum (Goldberg, 1989). For these reasons, the genetic algorithm was used to find the optimal locations and capacities of MR dampers in this study. Figure 4 provides a flow charft for the genetic algorithm used in this research.

To reduce the computational time, a preliminary study

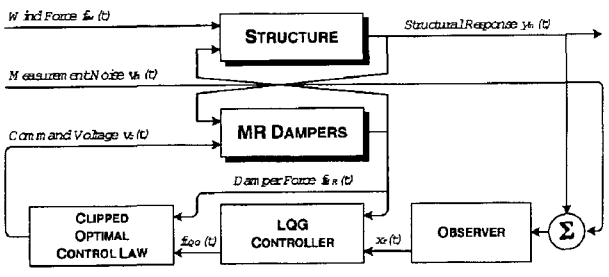

Fig. 3. Schematic Diagram for the Clipped Optimal Controller

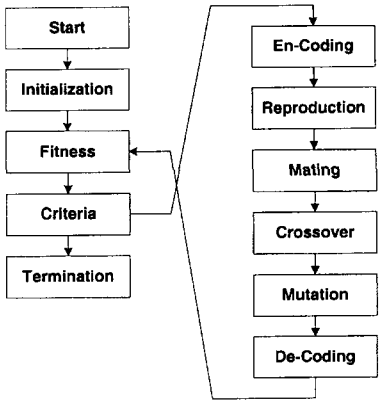

Fig. 4. Flow Chart of Genetic Algorithm

was carried out on 3 cases where 5 units of MR damper with the maximum capacity of 200 kN each placed o each floor and the dampers are operated passively (i.e. v_c(t = 0 Volt). They are Case 1 with MR dampers placed on th lower floors (3, 6, 10, 13, and 16th floors), Case 2 wit MR dampers placed on the middle (33, 36, 40, 43, and 46 th floors), and Case 3 with MR dampers placed on th higher floors (63, 66, 70, 73, and 76th floors). The result of the performance indices (described later in Section 4 shown in Table 2 indicate that it is more effective to plac the MR dampers at the higher floors. Therefore, only 6 66, 70, 73, and 76th floors were considered in determinin the capacities in terms of number of units using genet algorithm. The objective function was defined consid ering the performance criteria related to acceleration because the purpose of vibration control under wind load is mainly to reduce the discomfort of the occupants a

Table 2. Performance Indices for Three Different Dampe Locations

Criteria	MR Dampers (Passive off)		
	Case (1)	Case (2)	Case (3)
RMS Responses			
J_1	0.964	0.858	0.824
J_2	0.964	0.857	0.823
J_3	0.971	0.884	0.858
J_4	0.971	0.884	0.858
Peak Responses			
J_7	0.974	0.898	0.848
J_8	0.970	0.891	0.861
J_9	0.976	0.908	0.885
J_{10}	0.976	0.907	0.885

$$\begin{aligned} &argmax\ J(n_{MR,i}) = 4 - J_1 - J_2 - J_7 - J_8 \\ &n_{MR,i} \in \{0,1,2,3,4,5,6,7\} \\ &i \in \{63,66,70,73,76\} \end{aligned} \tag{11}$$

where J_1, J_2, J_7 and J_8 are the performance indices and $n_{MR,i}$ is the number of dampers on the i-th floor. Parameters for genetic algorithm are shown in Table 3. The optimum number of the MR damper units on each floor is determined as 2, 7, 5, 4, and 3 on 63, 66, 70, 73, and 76th floors, respectively. The present solution for the locations and the capacities of the MR dampers may be considered as an approximate optimum design. The true optimum design can be obtained by more elaborate analysis for many different cases.

4. Numerical Simulation Study

A numerical simulation study is carried out on the benchmark structure subjected to wind loads proposed by Yang, *et al.* (2000). It is a 76-story concrete office tower, and it is modeled as a system with 23 DOF's for structural analysis by the problem organizer. Detailed data related to this problem are given at the web site of the problem organizer. In this study, it is further reduced to a system with 5 DOFs (i.e. 10 dimensional state vector) using the state order reduction method for the computational efficiency in the control process.

Wind force data in along- and across-wind directions were determined from wind tunnel tests, which were performed by Samali *et al.* (1999). For this benchmark problem, 900 seconds of across-wind data are given for the computation of the structural response. In these wind data, the mean wind force on each floor has been removed, since it produces only the static deflection of the building. The reference mean wind speed, V_r, at the height of 10 meters above the ground is assumed to be 13.5 m/s, which represents to serviceability level related to the comfort of the occupants.

Ten performance criteria are related to the peak and RMS responses quantities, which can be obtained from the response time histories. Since the main objective is to reduce the absolute acceleration to alleviate the occupants discomfort, the first performance criterion for the controller is their ability to reduce the maximum floor RMS acceleration as:

Table 3. Parameters used in Genetic Algorithm

Parameter	Value	Parameter	Value
No. of variables	5	No. of population	30
Lower bound	0	No. of generation	15
Upper bound	7	Crossover Probability	0.9
Bits	3	Mutation Probability	0.005

$$J_1 = max(\sigma_{\ddot{y}1}, \sigma_{\ddot{y}30}, \sigma_{\ddot{y}50}, \sigma_{\ddot{y}55}, \sigma_{\ddot{y}60}, \sigma_{\ddot{y}65}, \sigma_{\ddot{y}70}, \sigma_{\ddot{y}75}) / \sigma_{\ddot{y}75o} \tag{12}$$

in which $\sigma_{\ddot{y}}$ and $\sigma_{\ddot{y}o}$ are the RMS accelerations of the i-th floor with and without control respectively. Acceleration of the 75th floor is considered, because it is the highest floor for the occupants. The second criterion is the average performance of acceleration for selected floors above the 49th floor as:

$$J_2 = \frac{1}{6}\sum_i (\sigma_{\ddot{y}} / \sigma_{\ddot{y}_{io}}) \tag{13}$$

for i = 50, 55, 60, 65, 70 and 75. The third and fourth evaluation criteria indicate the ability of the controllers to reduce the top floor displacements as:

$$J_3 = \sigma_{y76} / \sigma_{y76o} \tag{14}$$

$$J_4 = \frac{1}{7}\sum_i (\sigma_{yi} / \sigma_{yio}) \tag{15}$$

for i = 50, 55, 60, 65, 70, 75 and 76; in which σ_{yi} and σ_{yio} are the RMS displacements of the i-th floor with and without control respectively.

The performance criteria based on the peak response quantities are defined as:

$$J_7 = max(\ddot{y}_{p1}, \ddot{y}_{p30}, \ddot{y}_{p50}, \ddot{y}_{p55}, \ddot{y}_{p60}, \ddot{y}_{p65}, \ddot{y}_{p70}, \ddot{y}_{p75}) / \ddot{y}_{p75o} \tag{16}$$

$$J_8 = \frac{1}{6}\sum_i (\ddot{y}_{pi} / \ddot{y}_{pio}) \tag{17}$$

$$J_8 = \frac{1}{6}\sum_i (\ddot{y}_{pi} / \ddot{y}_{pio}) \tag{18}$$

$$J_9 = y_{p76} / y_{p76o} \tag{19}$$

$$J_{10} = \frac{1}{7}\sum_i (y_{pi} / y_{pio}) \tag{20}$$

for i = 50, 55, 60, 65, 70, 75 and 76; in which $\ddot{y}_{pi}, \ddot{y}_{pio}, y_{pi}$ and y_{pio} are the peak accelerations and displacements of the i-th floor with and without control. The smaller the index, the better the control performance. Figure 6 shows

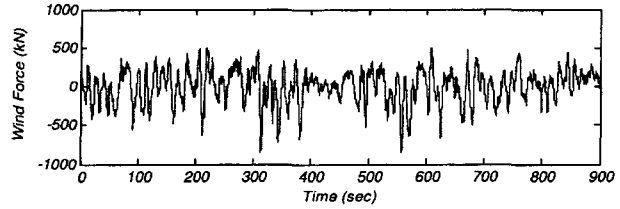

(a) Wind Force at 50th Floor

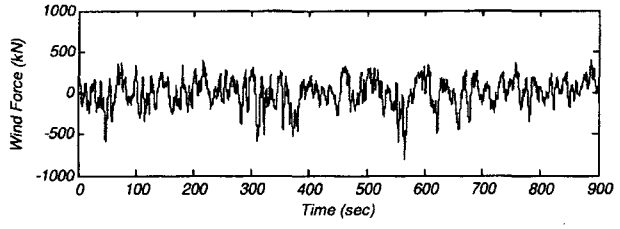

(a) Wind Force at 70th Floor r

Fig. 5. Time Histories of Wind Load at 50th and 70th Floors

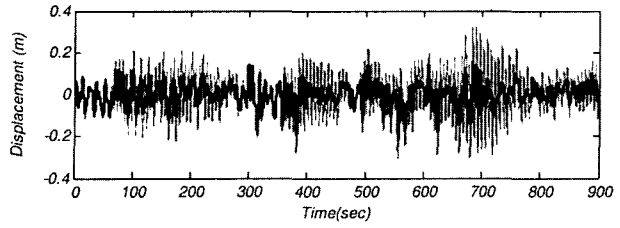

(a) Displacements of 76th floor

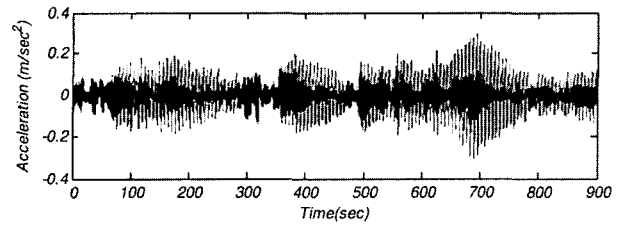

(b) Accelerations of 75th floor

Fig. 6. Time Histories of the Structural Responses with and without Semi-Active Control (Thin Line : Uncontrolled Case, Thick Line : Controlled Case)

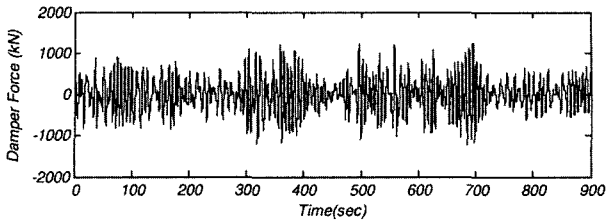

(a) Damper force at 66th floor

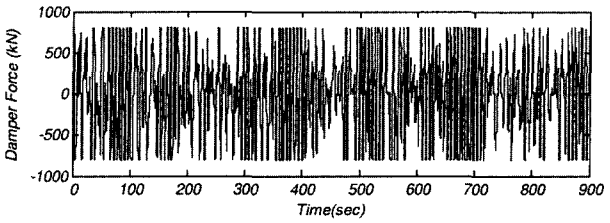

(b) Damper force at 73rd floor

Fig. 7. Time Histories of MR Damper Forces

time histories of structural responses with and without semi-active control, and Figure 7 shows time histories of the MR damper forces. The peak and RMS responses of the 76-story building with passive MR dampers and semi-actively controlled MR dampers are shown in Table 4 and Table 5. For simplicity only the responses of 30, 60, 75 and 76th floors are presented. Similar results for the cases with a tuned mass damper (TMD) and an active tuned mass damper (ATMD) obtained by Yang *et al.* (2000) are also shown for comparison. The performance indices for various control methods are compared in Table 6. The maximum damper forces are shown in Table 7. It is found that the semi-active control system employing MR dampers reduces the peak and RMS displacements of the building by 28-33% and 45-47% of the uncontrolled cases, and the peak and RMS acceleration by 49-58% and 61-65%. The improvement for the acceleration reduction is more significant, because the controllers are designed mainly for the reduction of the acceleration. The maximum allowable floor acceleration is 15 cm/sec² (or 5 cm/sec² in RMS

Table 4. Peak Response Quantities of 76-Story Building with Various Dampers

Floor	No Control		w/TMD		w/ATMD		w/MR Passive	Off	Clipped	Optimal
	y_{pi} cm	$\ddot{y}_{pi}$ cm/s²	y_{pi} cm	$\ddot{y}_{pi}$ cm/s²	y_{pi} cm	$\ddot{y}_{pi}$ cm/s²	y_{pi} Cm	$\ddot{y}_{pi}$ cm/s²	y_{pi} cm	$\ddot{y}_{pi}$ cm/s²
30	6.8	7.1	5.6	4.6	5.1	3.3	6.2	6.0	4.8	3.5
60	22.4	20.0	17.8	12.7	16.3	8.9	20.1	17.6	15.2	8.5
75	31.6	30.3	24.8	19.8	22.7	11.6	28.4	25.9	21.2	14.0
76	32.3	31.2	25.4	20.5	23.2	15.9	29.1	26.2	21.6	13.2

Table 5. RMS Response Quantities of 76-Story Building with Various Dampers

Floor	No Control		w/TMD		w/ATMD		w/MR Passive	Off	Clipped	Optimal
	σ_{yi} Cm	$\sigma_{\ddot{y}}$ cm/s^2	σ_{yi} cm	$\sigma_{\ddot{y}}$ cm/s^2	σ_{yi} cm	$\sigma_{\ddot{y}}$ cm/s^2	σ_{yi} Cm	$\sigma_{\ddot{y}}$ cm/s^2	σ_{yi} cm	$\sigma_{\ddot{y}}$ cm/s^2
30	2.25	2.02	1.48	1.23	1.26	0.89	1.89	1.71	1.17	0.77
60	7.02	6.42	4.79	3.72	4.08	2.81	6.15	5.42	3.77	2.28
75	9.92	9.14	6.75	5.38	5.74	3.34	8.67	7.72	5.29	3.52
76	10.10	9.35	6.90	5.48	5.86	4.70	8.87	7.89	5.41	3.41

Table 6. Control Performance Indices for Various Dampers

Criteria	w/ MR Dampers Passive Off	Clipped Optimal	w/TMD (Yang et al. 2000)	w/ATMD
J_1	0.84	0.38	0.58	0.36
J_2	0.84	0.36	0.58	0.41
J_3	0.87	0.53	0.68	0.57
J_4	0.87	0.53	0.68	0.58
J_7	0.85	0.46	0.65	0.38
J_8	0.88	0.44	0.63	0.43
J_9	0.90	0.66	0.78	0.71
J_{10}	0.90	0.67	0.79	0.72

Table 7. Maximum Damper Forces

Locations (Floor)	No. of Dampers	Forces (kN) Passive Off	Clipped Optimal
63	2	41.5	400.0
66	7	145.3	1261.3
70	5	105.1	1000.0
73	4	83.1	800.0
76	3	62.5	600.0

value), based on the design code for office buildings. It is observed that the semi-active control system with MR dampers satisfies the design requirement.

The performances of the semi-actively controlled MR dampers are found to be much better than those with a TMD, while they are fairly comparable to those with an ATMD. The performance indices of the MR dampers related to the peak accelerations (J_7 and J_8) are slightly higher than those with and ATMD, while the one related to the RMS acceleration (J_2) is slightly lower. Hysteresis curve of the MR damper on the 66th floor during the wind vibration control is shown in Figure 8.

The MR dampers are nonlinear devices, so their performance may vary significantly with the exciting force level. Thus, additional analyses are carried out on the case with the same control devices but for the different wind loads: i.e. $0.5\mathbf{f}_{ew}$, $1.5\mathbf{f}_{ew}$ and $2.0\mathbf{f}_{ew}$, $\mathbf{f}_{ew}$ where is the wind

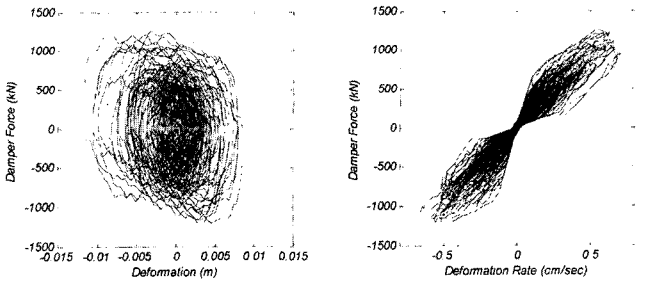

Fig. 8. Behavior of Semi-Actively Controlled MR Damper on 66th Floor

force for the case with V_r being 13.5 m/s. The performance indices are shown in Table 8 indicate that the semi-active control system with MR dampers is fairly robust to the variations of the exciting force level.

5. Conclusions

MR dampers are studied as semi-active control devices for a tall building subjected to wind loads. Clipped optimal control is used to control the strength of the magnetic filed applied to the dampers. Genetic algorithm is used for the optimal design of the controller locations and capacities. To verify the applicability of the MR dampers and the sug-

Table 8. Performance of MR Dampers for Various Wind Force Levels

Criteria	Force Levels $0.5\,\mathbf{f}_{ew}$	$\mathbf{f}_{ew}$	$1.5\,\mathbf{f}_{ew}$	$2.0\,\mathbf{f}_{ew}$
RMS Responses				
J_1	0.34	0.38	0.44	0.49
J_2	0.34	0.36	0.43	0.49
J_3	0.50	0.53	0.57	0.60
J_4	0.50	0.53	0.57	0.61
Peak Responses				
J_7	0.41	0.46	0.53	0.58
J_8	0.44	0.44	0.53	0.59
J_9	0.64	0.66	0.69	0.71
J_{10}	0.65	0.67	0.70	0.72

gested control algorithm, a numerical simulation study is carried out on the ASCE benchmark problem on wind vibration control of a tall building. The results of the present study are summarized as:

1. The semi-actively controlled MR dampers can effectively reduce both the peak and RMS responses due to wind excitation.
2. The genetic algorithm is effective for determining the optimal locations and capacities of the MR dampers.
3. The semi-active control system performs significantly better than the passive control systems.
4. The performance of the semi-active control system employing MR dampers is quite comparable to the performance of a control system with an active tuned mass damper.
5. The performance of the present semi-active control system is fairly robust against the vibrations of the wind force level.

Acknowledgements

The authors gratefully acknowledge the financial support to this research from the National Research Laboratory Project entitled "Development of Aseismic Control Technologies for Structures" sponsored by the Korea Institute of Science & Technology Evaluation and Planning (KISTEP) and from the National R&D Program by Ministry of Science and Technology of Korea.

References

Carlson JD, Weiss KD (1994) A growing attraction to magnetic fluids, Machine Design, 61-64.

Dyke SJ, Spencer BF, Sain MK, Carlson JD (1998) An experimental study of MR dampers for seismic protection, Smart Material and Structures (7): 693-703.

Goldberg DE (1989) Genetic Algorithms in Search, Optimization, and Machine Learning, Addison-Wiley.

Goodwin GC, Sin KS (1984) Adaptive Filtering, Prediction, and Control. Englewood Cliffs, New Jersey: Prentice-Hall.

Kim SB, Yun CB (2000) Sliding mode fuzzy control with disturbance estimator for wind-induced vibration control, Proc. of 2nd European Conference on Structural Control, Champ-Sur-Marne, France, 3-6 July 2000.

Koh HM, Park S, Park W, Park KS, Km YS (1998) Active vibration control of air traffic control tower at Inchon international airport under wind excitation, Proc. of the 2nd World Conference on Structural Control, Kyoto, Japan.

Spencer BF, Dyke SJ, Sain MK, Carlson JD (1997) Phenomenological model for magneto-rheological dampers, Journal of Engineering Mechanics, 230-238.

Spencer BF, Yang G, Carlson JD, Sain MK (1998) Smart dampers for seismic protection of structures: a full-scale study, Proc. of the 2nd World Conference on Structural Control, Kyoto, Japan.

Stanway R, Sproston JK, El-Wahed AK (1996) Application of electro-rheological fluids in vibration control: a survey, Smart Material and Structures 5(4): 464-482.

Symans MD, Constantinou MC (1999) Semi-active control systems for seismic protection of structures: a state-of-the-art review, Engineering Structures (21): 469-487.

Wereley NM, Pang L, Kamath GM (1998) Idealized hysterisis modeling of electro-rheological and magneto-rheological dampers, Journal of Intelligent Material Systems and Structures (9): 642-649.

Yang JN, Agrawal AK, Samali B, Wu JC (2000) A benchmark problem for response control of wind-excited tall buildings, Benchmark Problem Package Available at the World Wide Website: *http://gram.eng.uci.edu/civil/faculty/yang/index.html*

Yang JN, Samali B (1983) Control of tall buildings in along-wind motion, Journal of Engineering Mechanics, ASCE 121(12): 1330-1339.